JOURNAL OF SPACECRAFT AND ROCKETS
Vol. 39, No. 3, May–June 2002

Everything Is Relative in Spacecraft System Alignment Calibration

Mark E. Pittelkau*
Johns Hopkins University, Applied Physics Laboratory, Laurel, Maryland 20723

The concepts of absolute and relative alignment calibration of spacecraft attitude sensors are examined. It is known that three degrees of freedom of attitude associated with absolute alignment calibration are unobservable unless payload data are processed. It is shown that an absolute alignment model is equivalent to a relative alignment model when the payload is regarded as an attitude sensor. Then it is shown that the three unobservable degrees of freedom are eliminated by defining the gyro as the body reference frame, attributing only three nonorthogonal misalignment parameters to the gyro. The payload misalignment can then be parameterized and calibrated in the same manner as any attitude sensor, or this can be left strictly to the payload data processing, thus creating a well-defined boundary between attitude control system calibration and payload calibration. The new parameterization introduced is illustrated via simulation results.

Nomenclature

$A(\boldsymbol{q})$	=	attitude matrix corresponding to $\boldsymbol{q}$
$\boldsymbol{b}_g$	=	gyro bias vector, rad/s
C_q	=	payload measurement sensitivity to attitude perturbations
C_{δ_c}	=	payload measurement sensitivity to payload misalignment
H_c	=	payload measurement sensitivity matrix
$\boldsymbol{h}(\boldsymbol{x})$	=	payload measurement function
I	=	identity matrix of conforming dimension
P_c	=	payload attitude error covariance matrix
$\boldsymbol{p}$	=	payload measurement vector (unit vector)
$\boldsymbol{q}$	=	inertial-to-body attitude quaternion
T	=	Kalman filter measurement update interval, s
${}^{c}T_{co}(\boldsymbol{\delta}_c)$	=	payload misalignment transformation matrix corresponding to $\boldsymbol{\delta}_c$
${}^{co}T_b$	=	nominal transformation from body reference frame to the nominal (uncorrected) payload reference frame
${}^{go}T_b$	=	nominal transformation from body reference frame to the nominal (uncorrected) gyro reference frame
$U, \tilde{U}$	=	diagonal matrices of asymmetric scale factor errors
$\boldsymbol{x}$	=	Kalman filter perturbation state vector
$x_{\text{fp}}, y_{\text{fp}}$	=	payload focal plane measurements
$\Delta, \tilde{\Delta}$	=	general gyro misalignment matrices
$\boldsymbol{\delta}$	=	orthogonal gyro misalignment vector, rad
$\delta\boldsymbol{b}$	=	gyro bias perturbation vector, rad/s
$\boldsymbol{\delta}_c$	=	payload misalignment vector, rad
$\delta\boldsymbol{q}_v$	=	vector part of quaternion perturbation
$\boldsymbol{\delta}_{s1}$	=	star tracker 0 misalignment vector, rad
$\boldsymbol{\delta}_{s2}$	=	star tracker 1 misalignment vector, rad
$\delta_x, \delta_y, \delta_z$	=	orthogonal misalignments of the gyro (elements of $\boldsymbol{\delta}$)
$\boldsymbol{\eta}_a^2$	=	rate white noise
$\boldsymbol{\eta}_r^2$	=	angular acceleration white noise
$\Lambda, \tilde{\Lambda}$	=	diagonal matrices of symmetric scale factor errors
$\boldsymbol{\lambda}$	=	gyro symmetric scale factor error vector, nondimensional
$\lambda_x, \lambda_y, \lambda_z$	=	symmetric scale factor errors in the x, y, and z gyro axes (elements of $\boldsymbol{\lambda}$)
$\boldsymbol{\mu}$	=	gyro asymmetric scale factor error vector, nondimensional
μ_x, μ_y, μ_z	=	asymmetric scale factor errors in the x, y, and z gyro axes (elements of $\boldsymbol{\mu}$)
$\boldsymbol{\xi}$	=	gyro nonorthogonal misalignment vector, rad
ξ_x, ξ_y	=	nonorthogonal misalignments of the y-axis gyro about the x and y body axes, rad
ξ_z	=	nonorthogonal misalignments of the x-axis gyro about the z body axis, rad
σ_a^2	=	rate white noise variance
σ_r^2	=	angular acceleration white noise variance
Ω_g	=	gyro miscalibration sensitivity matrix
$\boldsymbol{\omega}_b$	=	true body angular rate vector, rad/s
$\boldsymbol{\omega}_{\text{gm}}$	=	gyro-measured angular rate, rad/s

Introduction

SENSOR alignment models necessarily fall into one of two categories: absolute or relative. For example, the alignment calibration models in Refs. 1–4 are of the absolute type, and the models in Refs. 5 and 6 are of the relative type. However, the authors of some of these papers evidently were not aware of the concepts of absolute and relative alignment or their implications.

The concepts of absolute and relative alignment calibration are clearly defined and analyzed in Refs. 7 and 8. As shown in Ref. 8, three orthogonal degrees of freedom of misalignment are unobservable in the absolute alignment model unless some other "absolute" attitude measurement is available such as payload data. Uncertainty in the unobservable degrees of freedom are bounded only by a priori information, which is usually of low accuracy when it is available. For many systems, postprocessing of payload data is required to produce a payload attitude measurement. This could impose a limitation on the availability and usefulness of payload data for system alignment calibration and requires an interface between payload scientists and attitude control system (ACS) engineers. Such an interface is often not practical because it demands more extensive system engineering to define requirements, it requires a payload telemetry interface and payload data processing, and it can create logistical problems with data storage and retrieval in the ground processing system. In addition, the ACS engineers are often unavailable once a payload is in full operation, which may be a problem in systems that require periodic recalibration. Subtle problems could also occur such as the random walk divergence of calibration parameters described in Ref. 9.

We seek a general and unified approach to system calibration that eliminates complications associated with absolute alignment calibration. In addition to the attitude sensor alignment calibration, we also want to estimate alignment and other calibration parameters

Received 28 February 2001; revision received 27 November 2001; accepted for publication 29 November 2001.

*Senior Staff Engineer, Space Department, 11100 Johns Hopkins Road; mark.pittelkau@jhuapl.edu. Senior Member AIAA.

for a gyro assembly.[1,10] In this paper, we will refer to a gyro assembly that senses angular rate in three orthogonal directions as simply "the gyro" instead of referring to it by one of many common acronyms.

The following example will serve to illustrate the relationship between absolute and relative alignment. The alignment Kalman filter developed in Ref. 1 is based on an absolute alignment calibration model comprising an alignment vector for each of two star trackers, a general six-parameter gyro alignment model (two degrees of freedom for each of three gyro axes), and gyro bias and scale factor parameters. The a priori sensor alignment is measured with respect to a master reference cube (MRC) that nominally defines the body reference frame. (The MRC is a very accurate optical cube used for alignment measurement.) Three degrees of freedom of alignment are unobservable in this model. Observability is obtained, and the absolute misalignment is estimated by processing attitude measurements from the payload. The payload orientation with respect to the MRC is not parameterized with misalignment parameters, otherwise there would still be three extra degrees of freedom. The body reference frame is effectively transferred from the MRC to the payload when the absolute alignment error is estimated; the MRC becomes an unimportant intermediate reference frame.

In effect, we have n attitude sensors including the payload ($n = 4$ in the system just described) but only $n - 1$ orientation error vectors to estimate. The absolute alignment model becomes a relative alignment model with the inclusion of the payload as an attitude sensor. Clearly we could model any subset of $n - 1$ sensors with misalignment vectors. The remaining sensor is called the *reference sensor* because it effectively defines the body reference frame; all other sensors are aligned relative to the reference sensor. Thus, we can dispense with the notion of absolute alignment; everything is relative in alignment calibration.

The payload is an inappropriate choice for the reference sensor for practical reasons already discussed. One obvious choice of reference sensor is one of the star trackers. The orientation of each of the other sensors is relative to that star tracker. This model is not satisfactory because measurements might not always be available from the tracker used as the reference sensor. The star tracker's physical axes are also not a convenient reference.

An orthogonal set of axes defined by the gyros has traditionally been considered the body reference frame in attitude determination filters. In addition, gyro data are available continuously. Hence, it makes sense to consider the gyro as the reference sensor in a relative alignment model. How this is done is a novelty of the development in this paper.

The general six-parameter gyro misalignment model in Ref. 1 can be factored as a product of orthogonal and nonorthogonal misalignment matrices as shown in the next section. The orthogonal misalignment is then set to zero to eliminate three degrees of freedom. The body frame is, thus, defined by the gyro axes corrected for nonorthogonal misalignment and possibly for some known and fixed mounting orientation. The star tracker and payload misalignments relative to the gyro can then be modeled and estimated. Omitting the payload and its misalignment vector from the model does not affect the observability of the remaining vectors because all other sensor alignments are modeled relative to the reference sensor, which is defined by the orthogonal gyro frame.

Internal-to-external orthogonal misalignment and orthogonal mounting misalignment of the gyro are estimated as part of the misalignment of the other sensors because the alignment of all sensors is relative to the gyro frame. For gyros that come with three single-axis sensing units mounted internally to a package, the internal-to-external misalignment is usually calibrated by the manufacturer with fair accuracy and can be used to reduce uncertainty in the initial misalignment estimate.

The relative alignment calibration model described will be illustrated by a system in which there are two star trackers, three single-axis gyros mounted nearly orthogonally, and an imaging sensor that operates intermittently over an orbit. A set of payload pointing measurements may be derived from the imaging sensor data by identifying surveyed landmarks in the image. Alternatively, the payload misalignment with respect to the attitude determination system can be determined directly as part of the image processing. In either approach, the estimated attitude history is required in the image processing. The surveyed landmarks are required for payload alignment calibration. In any practical global imaging system, such landmarks are not generally available, and so this type of payload is not a good choice for a reference sensor in an alignment calibration model.

In the next section, we derive a mathematical description of the relative alignment parameterization. This is done first for the gyro and then for the payload. The alignment parameterization and the measurement sensitivity matrix of the star tracker were developed in Ref. 1 and will not be repeated here. A square root Kalman filter implementation, called an alignment Kalman filter or AKF, was also presented there. We will refer to the calibration algorithm in this paper as an AKF also. A detailed exposition of the implementation of the relative alignment calibration model is beyond the scope of this paper. However, some notes are given to describe how its implementation differs from that of the absolute alignment calibration model in Ref. 1, where substantial detail can be found.

Relative Alignment Parameterization

A parameterization of the gyro misalignment for relative alignment calibration is given in the following subsection. Other gyro calibration parameters are also introduced. The measurement sensitivity matrix for the payload attitude measurement is derived in the subsequent subsection.

The state vector for most attitude determination filters[11] comprises attitude perturbation and gyro bias perturbation states $\delta\boldsymbol{q}_v$ and $\delta\boldsymbol{b}$. The state vector for the AKF comprises these states and also various calibration parameters. The calibration parameters considered and defined subsequently are a vector $\boldsymbol{\xi}$ of three parameters for nonorthogonal misalignment of the gyro axes, a symmetric scale factor vector $\boldsymbol{\lambda}$ for each sensing axis, an asymmetric scale factor vector $\boldsymbol{\mu}$ for each sensing axis, two misalignment vectors for the two star trackers, and a misalignment vector for the payload. The state vector is then

$$\boldsymbol{x} = \left(\delta\boldsymbol{q}_v^T, \delta\boldsymbol{b}^T, \boldsymbol{\xi}^T, \boldsymbol{\lambda}^T, \boldsymbol{\mu}^T, \boldsymbol{\delta}_{s1}^T, \boldsymbol{\delta}_{s2}^T, \boldsymbol{\delta}_c^T\right)^T \tag{1}$$

Gyro Calibration Model

The gyro-measured angular rate vector $\boldsymbol{\omega}_{\text{gm}}$ is related to the true angular rate vector $\boldsymbol{\omega}_b$ (in body coordinates) by

$$\boldsymbol{\omega}_{\text{gm}} = (I - \tilde{\Lambda} - \tilde{U})(I - \tilde{\Delta})^{g_o}T_b\boldsymbol{\omega}_b - \boldsymbol{b}_g - \boldsymbol{\eta}_a \tag{2}$$

where $\boldsymbol{b}_g$ is gyro bias (in gyro coordinates) and $\boldsymbol{\eta}_a$ is a rate white noise with covariance $\sigma_{\eta_a}^2 I$. (Note that $\sigma_{\eta_a}^2$ is popularly but incorrectly called the angle random walk variance.) Here $\boldsymbol{\omega}_b$ is the true angular rate in body coordinates, ${}^{g_o}T_b$ is the transformation matrix describing the nominal orientation of the gyro reference frame g_o with respect to the body coordinate system b, $\boldsymbol{\omega}_{\text{gm}}$ is in the gyro frame g_o, $I - \tilde{\Delta}$ is a nonorthogonal small angle misalignment matrix, $\tilde{\Lambda} = \text{diag}(\lambda_x, \lambda_y, \lambda_z)$ is a diagonal matrix of symmetric scale factor errors, and $\tilde{U} = \text{diag}[\mu_x \text{ sign}(\omega_x), \mu_y \text{ sign}(\omega_y), \mu_z \text{ sign}(\omega_z)]$ is a diagonal matrix of asymmetric scale factor errors, where sign$(\cdot)$ returns the sign of its argument. [Vector elements are denoted by subscripts x, y, and z, for example, $\boldsymbol{\omega} = (\omega_x, \omega_y, \omega_z)^T$.] Note that asymmetric scale factor errors can be important if, for example, a fiber optic gyro is used and much less so if a ring laser gyro is used.

The bias is modeled as a rate random walk process, or drift, $\dot{\boldsymbol{b}}_g = \boldsymbol{\eta}_r$, where $\boldsymbol{\eta}_r$ is an angular acceleration white noise process with covariance $\sigma_{\eta_r}^2 I$. (Note that $\sigma_{\eta_r}^2$ is popularly but incorrectly called the rate random walk variance.) This variance is computed from the drift variance typically quoted by gyro manufacturers as $\sigma_{\eta_r}^2 = (2/\tau_d)\sigma_d^2$, where τ_d is the specified drift stability interval.

The true angular rate is obtained by solving Eq. (2) for $\boldsymbol{\omega}_b$. Then

$$\begin{aligned}\boldsymbol{\omega}_b &= {}^bT_{g_o}(I - \tilde{\Delta})^{-1}(I - \tilde{\Lambda} - \tilde{U})^{-1}(\boldsymbol{\omega}_{\text{gm}} + \boldsymbol{b}_g + \boldsymbol{\eta}_a)\\ &= {}^bT_{g_o}(I + \Delta)(I + \Lambda + U)(\boldsymbol{\omega}_{\text{gm}} + \boldsymbol{b}_g + \boldsymbol{\eta}_a)\\ &\simeq {}^bT_{g_o}(I + \Delta + \Lambda + U)(\boldsymbol{\omega}_{\text{gm}} + \boldsymbol{b}_g + \boldsymbol{\eta}_a)\end{aligned} \tag{3}$$

Note that $\Delta \simeq \tilde{\Delta}$, $\Lambda \simeq \tilde{\Lambda}$, and $U \simeq \tilde{U}$ because the misalignments and scale factor errors are small.

Because each sensing axis of the gyro is misaligned independently of the others, the misalignment matrix $I+\Delta$ is defined by the sum of orthogonal small-angle rotations of the true angular rate vector about each axis. Each rotation is approximated by a matrix of the form $I+[\boldsymbol{\delta}_i\times]$, where $i\in\{x,y,z\}$ is an axis label. Let $\boldsymbol{\omega}'=(I+\Lambda)\boldsymbol{\omega}$ and $\boldsymbol{\omega}=\boldsymbol{\omega}_{\text{gm}}+\boldsymbol{b}_g+\boldsymbol{\eta}_a$. The gyro rate in the misaligned coordinate system is

$$
\begin{aligned}
{}^{go}T_b\boldsymbol{\omega}_b=(I+\Delta)\boldsymbol{\omega}'&=\begin{bmatrix}1&-\delta_{xz}&\delta_{xy}\\ \delta_{xz}&1&0\\ -\delta_{xy}&0&1\end{bmatrix}\begin{bmatrix}\omega_x'\\0\\0\end{bmatrix}\\
&+\begin{bmatrix}1&-\delta_{yz}&0\\ \delta_{yz}&1&-\delta_{yx}\\ 0&\delta_{yx}&1\end{bmatrix}\begin{bmatrix}0\\ \omega_y'\\0\end{bmatrix}+\begin{bmatrix}1&0&\delta_{zy}\\ 0&1&-\delta_{zx}\\ -\delta_{zy}&\delta_{zx}&1\end{bmatrix}\begin{bmatrix}0\\0\\ \omega_z'\end{bmatrix}\\
&=\begin{bmatrix}1&-\delta_{yz}&\delta_{zy}\\ \delta_{xz}&1&-\delta_{zx}\\ -\delta_{xy}&\delta_{yx}&1\end{bmatrix}\begin{bmatrix}\omega_x'\\ \omega_y'\\ \omega_z'\end{bmatrix}
\end{aligned}
\tag{4}
$$

The matrix $I+\Delta$ can be factored such that $I+\Delta=\mathcal{Q}\mathcal{R}$, where $\mathcal{Q}$ is orthogonal and $\mathcal{R}$ is upper triangular. The matrix $\mathcal{Q}$ is well approximated by a small-angle transformation $I+[\boldsymbol{\delta}\times]$ and $\mathcal{R}$ by three nonorthogonal misalignment angles ξ_x, ξ_y, and ξ_z. Then

$$
\begin{aligned}
I+\Delta=(I+[\boldsymbol{\delta}\times])\mathcal{R}&=\begin{bmatrix}1&-\delta_z&\delta_y\\ \delta_z&1&-\delta_x\\ -\delta_y&\delta_x&1\end{bmatrix}\begin{bmatrix}1&\xi_z&-\xi_y\\0&1&\xi_x\\0&0&1\end{bmatrix}\\
&\simeq\begin{bmatrix}1&-(\delta_z-\xi_z)&\delta_y-\xi_y\\ \delta_z&1&-(\delta_x-\xi_x)\\ -\delta_y&\delta_x&1\end{bmatrix}
\end{aligned}
\tag{5}
$$

where ξ_x, ξ_y, and ξ_z are elements of the nonorthogonal matrix $\mathcal{R}$. Equating like terms with the misalignment matrix in Eq. (4) yields the orthogonal and nonorthogonal misalignments in terms of the general misalignments:

$$\delta_x=\delta_{yx},\qquad \xi_x=\delta_{yx}-\delta_{zx} \tag{6a}$$

$$\delta_y=\delta_{xy},\qquad \xi_y=\delta_{xy}-\delta_{zy} \tag{6b}$$

$$\delta_z=\delta_{xz},\qquad \xi_z=\delta_{xz}-\delta_{yz} \tag{6c}$$

This result provides an alternative means of parameterizing the general gyro misalignment model in Eq. (4) whereby the orthogonal and nonorthogonal misalignments are distinct in the model.

A similar result is obtained by computing the $\mathcal{Q}\mathcal{S}$ factorization of $I+\Delta$, where $\mathcal{S}$ is symmetric. This is derived in the Appendix. Other factorizations are not pursued in this paper. The choice of factorization is only one of convenience; the $\mathcal{Q}\mathcal{R}$ factorization makes it somewhat easier to compute the upper-diagonal (UD) factors of the process noise matrix.

Setting the orthogonal misalignment $\boldsymbol{\delta}$ to zero ($\delta_x=\delta_y=\delta_z=0$) gives $I+\Delta=\mathcal{R}$. This removes three unobservable degrees of freedom of attitude and defines the gyro as the reference sensor. Because the coefficients are states to be estimated, we get from Eq. (3) and noting that $U\omega=(\mu_x|\omega_x|,\mu_y|\omega_y|,\mu_z|\omega_z|)^T$,

$$
\begin{aligned}
\boldsymbol{\omega}_b&={}^bT_{go}\boldsymbol{\omega}_{\text{gm}}+{}^bT_{go}(I+\Delta+\Lambda+U)(\boldsymbol{b}_g+\boldsymbol{\eta}_a)+{}^bT_{go}\\
&\times\begin{bmatrix}0&-\omega_z&\omega_y&\omega_x&0&0&|\omega_x|&0&0\\ \omega_z&0&0&0&\omega_y&0&0&|\omega_y|&0\\ 0&0&0&0&0&\omega_z&0&0&|\omega_z|\end{bmatrix}\begin{bmatrix}\xi_x\\ \xi_y\\ \xi_z\\ \lambda_x\\ \lambda_y\\ \lambda_z\\ \mu_x\\ \mu_y\\ \mu_z\end{bmatrix}
\end{aligned}
\tag{7}
$$

$$\simeq{}^bT_{go}\boldsymbol{\omega}_{\text{gm}}+{}^bT_{go}\boldsymbol{b}_g+{}^bT_{go}\Omega_g\boldsymbol{\delta}_g+{}^bT_{go}\boldsymbol{\eta}_a \tag{8}$$

with the obvious identification of the matrix Ω_g and the vector $\boldsymbol{\delta}_g$ from Eq. (7). Equation (8) is part of the state model to be implemented in an extended Kalman filter to estimate the calibration parameters.

Payload Alignment Calibration Model

Although alignment calibration of the payload is optional in the relative alignment error model, the following derivations apply to any vector sensor, such as a sun sensor, that may require calibration.

The payload considered here produces a measurement vector

$$\boldsymbol{h}(\boldsymbol{x})=\begin{bmatrix}x_{\text{fp}}\\ y_{\text{fp}}\end{bmatrix}=\begin{bmatrix}p_x/p_z\\ p_y/p_z\end{bmatrix} \tag{9}$$

where ${}^c\boldsymbol{p}=(p_x,p_y,p_z)^T$ is a unit vector in payload coordinates, x_{fp} and y_{fp} are measured along orthogonal axes in the focal plane of the sensor, and the state vector $\boldsymbol{x}$ was defined in Eq. (1). Several reference vectors are available when a calibration target is in view of the payload. The reference vector ${}^i\boldsymbol{p}$ in inertial coordinates is transformed to the payload frame by

$${}^c\boldsymbol{p}(\boldsymbol{q},\boldsymbol{\delta}_c)={}^cT_{co}(\boldsymbol{\delta}_c){}^{co}T_bA(\boldsymbol{q}){}^i\boldsymbol{p} \tag{10}$$

where ${}^cT_{co}(\boldsymbol{\delta}_c)=I-[\boldsymbol{\delta}_c\times]$ is a misalignment matrix parameterized by the small angle rotation vector $\boldsymbol{\delta}_c$, ${}^{co}T_b$ is the nominal body-to-sensor mounting matrix, and $A(\boldsymbol{q})$ is the attitude matrix corresponding to the attitude quaternion $\boldsymbol{q}$, which describes the body attitude with respect to the inertial reference frame.

Following the derivation of the general measurement sensitivity matrix in Ref. 11 for vector measurements, we have the payload attitude measurement sensitivity matrix

$$H_c=\frac{\partial\boldsymbol{h}}{\partial\boldsymbol{x}}=\begin{bmatrix}C_q&\boldsymbol{0}&C_{\delta_c}\end{bmatrix} \tag{11}$$

where

$$C_q=\frac{\partial\boldsymbol{h}}{\partial\delta\boldsymbol{q}_v}=2\boldsymbol{r}^T[{}^b\boldsymbol{p}\times] \tag{12a}$$

$$\boldsymbol{r}^T=\frac{\partial\boldsymbol{h}}{\partial{}^c\boldsymbol{p}}{}^cT_{co}(\boldsymbol{\delta}_c){}^{co}T_b \tag{12b}$$

$${}^b\boldsymbol{p}=A(\boldsymbol{q}){}^i\boldsymbol{p} \tag{12c}$$

and where

$$C_{\delta_c}=\frac{\partial\boldsymbol{h}}{\partial\boldsymbol{\delta}_c}=\boldsymbol{s}^T[{}^c\boldsymbol{p}\times] \tag{13a}$$

$$\boldsymbol{s}^T=\frac{\partial\boldsymbol{h}}{\partial{}^c\boldsymbol{p}} \tag{13b}$$

$${}^c\boldsymbol{p}={}^cT_{co}(\boldsymbol{\delta}_c){}^{co}T_bA(\boldsymbol{q}){}^i\boldsymbol{p} \tag{13c}$$

From Eq. (12b),

$$
\begin{aligned}
\boldsymbol{r}^T=\begin{bmatrix}\boldsymbol{r}_x^T\\ \boldsymbol{r}_y^T\end{bmatrix}=\frac{\partial\boldsymbol{h}}{\partial{}^c\boldsymbol{p}}{}^cT_{co}{}^{co}T_b&=\begin{bmatrix}\dfrac{\partial x_{\text{fp}}}{\partial p_x}&\dfrac{\partial x_{\text{fp}}}{\partial p_y}&\dfrac{\partial x_{\text{fp}}}{\partial p_z}\\ \dfrac{\partial y_{\text{fp}}}{\partial p_x}&\dfrac{\partial y_{\text{fp}}}{\partial p_y}&\dfrac{\partial y_{\text{fp}}}{\partial p_z}\end{bmatrix}{}^cT_{co}{}^{co}T_b\\
&=\begin{bmatrix}\dfrac{1}{p_z}&0&-\dfrac{p_x}{p_z^2}\\ 0&\dfrac{1}{p_z}&-\dfrac{p_y}{p_z^2}\end{bmatrix}{}^cT_{co}{}^{co}T_b
\end{aligned}
\tag{14}
$$

where p_x, p_y, and p_z are elements of the vector ${}^c\boldsymbol{p}$. Then from Eq. (12a), C_q is given by

$$C_q=\begin{bmatrix}2\left(\boldsymbol{r}_x\times{}^b\boldsymbol{p}\right)^T\\ 2\left(\boldsymbol{r}_y\times{}^b\boldsymbol{p}\right)^T\end{bmatrix} \tag{15}$$

Similarly, from Eq. (13b), we get

$$s^T = \begin{bmatrix} s_x^T \\ s_y^T \end{bmatrix} = \begin{bmatrix} 1/p_z & 0 & -p_x/p_z^2 \\ 0 & 1/p_z & -p_y/p_z^2 \end{bmatrix} \tag{16}$$

Then from Eq. (13a) C_{δ_c} is given by

$$C_{\delta_c} = \begin{bmatrix} (s_x \times {}^c\boldsymbol{p})^T \\ (s_y \times {}^c\boldsymbol{p})^T \end{bmatrix} \tag{17}$$

The measurement residuals are given by

$$v_x = x_{\text{fpm}} - p_x/p_z, \qquad v_y = y_{\text{fpm}} - p_y/p_z \tag{18}$$

where x_{fpm} and y_{fpm} are measured in the focal plane of the sensor. The Jacobian matrices C_q and C_{δ_c}, the matrices $\boldsymbol{r}$ and $\boldsymbol{s}$, and the reference vectors ${}^b\boldsymbol{p}$ and ${}^c\boldsymbol{p}$ are evaluated at the a priori estimates $\hat{\boldsymbol{q}}^-$ and $\hat{\boldsymbol{\delta}}_c^-$.

Remark: In the absolute alignment model in Ref. 1, the body reference frame is effectively the payload reference frame, and so the covariance of the payload pointing error is given by the attitude error covariance. In the relative alignment model, the covariance of the payload pointing error is given by

$$P_c = H_c P H_c^T \tag{19}$$

where $P = UDU^T$ is the filter error covariance matrix and U and D are its UD factors. Of course we rarely want to compute P in a UD implementation. The payload pointing error covariance is easily computed from $H_c P H_c^T = H_c UD U^T H_c^T = (H_c U) D (H_c U)^T$. The computation is even simpler when only the main diagonal of P_c is needed. It should be obvious that the diagonal elements of P_c will be greater than the corresponding body attitude error variances in P because P_c reflects payload misalignment uncertainty in addition to uncertainty in the estimated attitude of the body reference frame. When there are no payload measurements, the payload misalignment is essentially the same as the unobservable degrees of freedom in the absolute alignment error model. Neglecting the unobservable degrees of freedom when computing the attitude uncertainty (in this case the payload attitude uncertainty) is called "naive" in Ref. 8 because the attitude uncertainty is believed to be much smaller (as indicated by the first three diagonal elements of P) than it truly is (as indicated by the diagonal elements of P_c).

Implementation Note

The calibration algorithm is implemented by using the UD factorization algorithm described in Ref. 1, where the block structure of the process noise matrix was used to obtain a simple algorithm to compute its factorization. The Ω_g matrix in Eq. (8) does not exhibit such a structure. This difficulty is circumvented by defining a permutation vector that identifies which columns contain nonzero entries for the x, y, and z axes and another vector that contains these entries. Simplicity is regained with this approach. Further implementation details are beyond the scope of this paper.

Mitigating Gyro Calibration Errors

A real-time on-orbit attitude determination filter usually estimates only attitude and gyro bias, and so the real-time filter will exhibit degraded performance in the presence of residual calibration error.[1] A process noise matrix that this author calls a cover covariance can substantially reduce the degradation of performance (Ref. 12, pp. 305, 306). This was derived and demonstrated in Ref. 1. A slightly modified derivation is given here for the relative alignment error model. Because the misalignments and scale factor errors in the gyro model Eq. (8) are not estimated in the on-orbit Kalman filter, they can be retained as process noise inputs to the following attitude and bias model:

$$\begin{bmatrix} \delta\boldsymbol{q}_v \\ \delta\boldsymbol{b}_g \end{bmatrix}_{k+1} = \begin{bmatrix} \phi_k & \frac{1}{2}\gamma_k {}^bT_{g_o} \\ 0 & I \end{bmatrix} \begin{bmatrix} \delta\boldsymbol{q}_v \\ \delta\boldsymbol{b}_g \end{bmatrix}_k + \Gamma_k' \boldsymbol{\eta}_k' + \frac{1}{2}\gamma_k {}^bT_g \Omega_{g_0} \boldsymbol{\delta}_g \tag{20}$$

where ϕ_k and γ_k are elements of the state transition matrix, $\delta\boldsymbol{q}_v$ and $\delta\boldsymbol{b}_g$ are perturbation states (from linearization), and $\boldsymbol{\eta}_k'$ is a discrete white process noise with $\mathcal{E}\{\boldsymbol{\eta}_k'\boldsymbol{\eta}_k'^T\} = I$. The matrix Γ_k' is a square root of the process noise matrix for the filter. The gyro parameter vector $\boldsymbol{\delta}_g$ can be treated as a white random process with covariance

$$\Sigma_g = \alpha^2 \operatorname{diag}\left(\sigma_{yz}^2, \sigma_{zy}^2, \sigma_{zx}^2, \sigma_{\lambda x}^2, \sigma_{\lambda y}^2, \sigma_{\lambda z}^2, \sigma_{\mu x}^2, \sigma_{\mu y}^2, \sigma_{\mu z}^2\right) \tag{21}$$

where α is a scalar tuning parameter. With the approximation $\gamma_k = TI$, where T is the prediction time, the covariance of the last term in Eq. (20) is given by the cover covariance matrix

$$Q_{cc} = (T^2/4) {}^bT_{g_o} \Omega_g \Sigma_g \Omega_g^T {}^bT_{g_o}^T$$

Let $\sigma_x^2 = \sigma_{\lambda x}^2 + \sigma_{\mu x}^2$, $\sigma_y^2 = \sigma_{\lambda y}^2 + \sigma_{\mu y}^2$, $\sigma_z^2 = \sigma_{\lambda z}^2 + \sigma_{\mu z}^2$. Expanding the equation for Q_{cc} gives the very simple expression for the cover covariance

$$Q_{cc} = \alpha^2 \frac{T^2}{4} {}^bT_{g_o} \times \begin{bmatrix} \omega_x^2\sigma_x^2 + \omega_y^2\sigma_{yz}^2 + \omega_z^2\sigma_{zy}^2 & 0 & 0 \\ 0 & \omega_y^2\sigma_y^2 + \omega_z^2\sigma_{zx}^2 & 0 \\ 0 & 0 & \omega_z^2\sigma_z^2 \end{bmatrix} {}^bT_{g_o}^T \tag{22}$$

where $\boldsymbol{\omega} = \boldsymbol{\omega}_{\text{gm}} + \hat{\boldsymbol{b}}_g$ is the bias-corrected gyro measurement. Because this matrix depends on angular rate, the cover covariance is large only for large angular rates where the effect of the miscalibration is more pronounced. Note that $\boldsymbol{\omega}$ and $\hat{\boldsymbol{b}}$ are in body coordinates if the gyro-to-body reference frame transformation ${}^bT_{g_o}$ is omitted from the preceding equations.

A cover covariance for attitude sensor misalignments can be added to the measurement covariance matrix. Because the relative misalignment model eliminates unobservable degrees of freedom that exist in the absolute misalignment model, the cover covariance for the relative alignment model requires less process noise and, therefore, gives better results than were shown in Ref. 1 for the absolute alignment model.

Simulation Results

The model parameters that were used to generate the results in this section are the same as in Ref. 1 except that here the orthogonal misalignment of the gyro is zero, asymmetric scale factor errors are included in the present gyro calibration model, and the payload is misaligned with respect to the body reference frame. The asymmetric scale factors are also introduced. The following data are realistic for an attitude determination system. The star tracker misalignment vectors are $\boldsymbol{\delta}_{s1} = (-20, -20, 20)^T$ and $\boldsymbol{\delta}_{s2} = (20, 20, 20)^T$ arc-s. The symmetric scale factor vector of the gyro is $\boldsymbol{\lambda} = (500, 500, 500)^T$ ppm, and the asymmetric scale factor vector is $\boldsymbol{\mu} = (500, 500, 500)^T$ ppm. The gyro misalignments are $\delta_x = \delta_y = \delta_z = 0$, that is, $\delta_{xz} = \delta_{xy} = \delta_{yx} = 0$, and $\xi = (-400, -300, -200)^T$ arc-s, that is, $\delta_{zx} = 400$, $\delta_{zy} = 300$, and $\delta_{yz} = 200$). The 1σ star tracker accuracy is 6 arc-s in the cross boresight axes and 37 arc-s in the boresight axis. The standard deviation of the rate white noise of the gyros is 0.005 deg/$\sqrt{h}$ and their 1σ drift stability is 0.05 deg/h over 1000 s. The 1σ attitude measurement accuracy of the payload is 0.5 arc-s in each of the two cross-boresight directions, and it has a 1-deg field of view. The filter's measurement update interval is 0.2 s. Finally, the calibration maneuver is a 0.5-deg/s sinusoid that varies at 0.01, 0.0085, and 0.008 Hz in the x, y, and z axes, respectively.

Figures 1a–1h show the performance of the relative alignment estimator. These graphs show the estimation errors and the $\pm 1\sigma$ bounds computed from the filter's covariance matrix. Payload attitude measurements were taken at 5 Hz for 100 s starting at 500 s and again for 100 s starting at 1000 s. These results show that all parameters converge, except the payload misalignments, before processing payload measurements of attitude. The payload misalignment estimate converges only when payload attitude measurements are

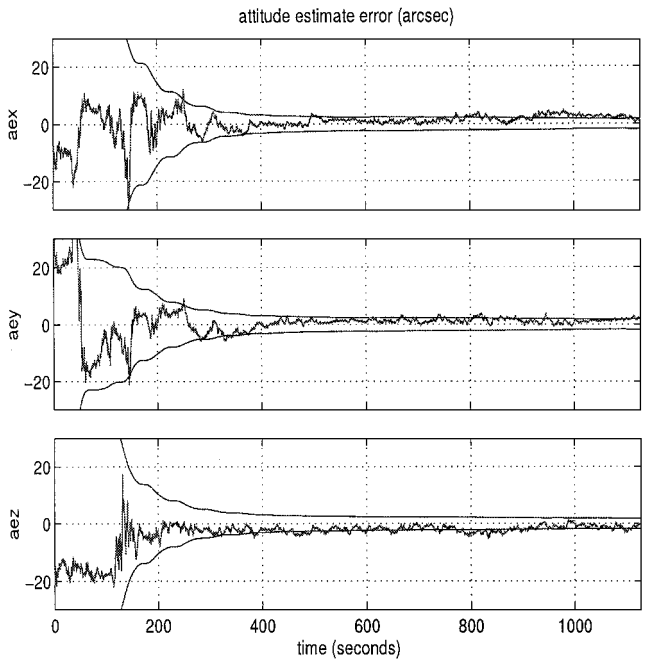

a) Attitude estimate error (arc-s)

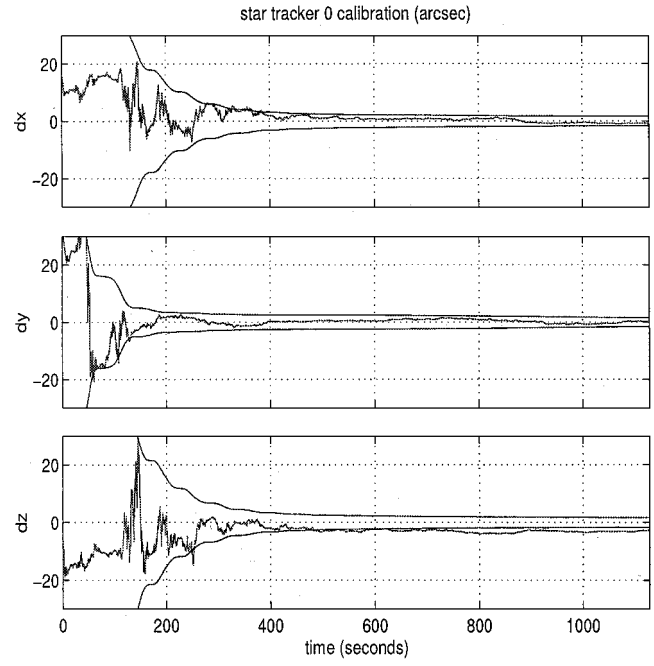

c) Star tracker 0 alignment estimation error (arc-s)

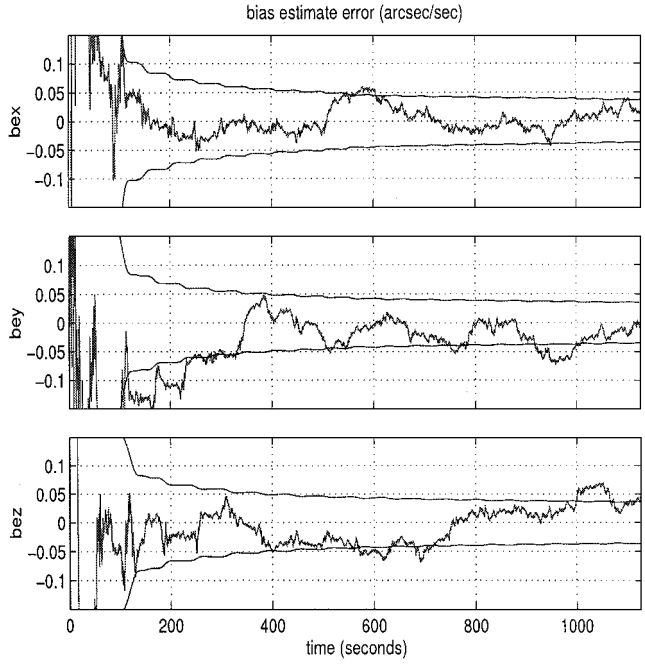

b) Gyro bias estimation error (deg/h)

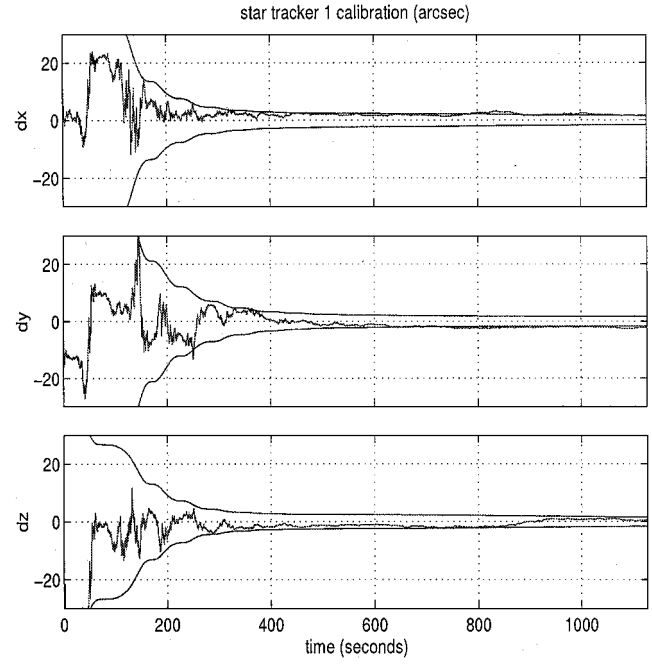

d) Star tracker 1 alignment estimation error (arc-s)

Fig. 1 Relative alignment calibration results.

processed. The processing of payload measurements does not substantially affect the estimation of the other calibration parameters, although a change in the estimated asymmetric scale factor error in Fig. 1f appears to coincide with the processing of the payload attitude measurements. (The meandering of estimation errors outside of the 1σ bounds is not an indication of divergence or bias, rather it is simply a result of the estimation errors having a long correlation time.) Note from Figs. 1a–1c and 1f that the attitude and misalignment parameter estimates of the star trackers converge as the nonorthogonal misalignment parameter estimates of the gyro converge. Their rate of convergence depends on the angular rate of the spacecraft as well as the accuracy of the gyros and star trackers. To the author's knowledge, a study of this empirical fact has not appeared in the literature. However, a method to combine estimates from individual calibrations of low quality due to limited maneuvers is presented in Ref. 13.

The reader should compare these results with those of the absolute alignment estimator presented in Ref. 1. In that estimator, the convergence of attitude and of the misalignment parameters is limited by the absolute alignment error until payload data is processed and is ultimately limited by the quality and quantity of payload data. The convergence of the absolute alignment error in Ref. 1 is similar to the convergence of the payload misalignment in Fig. 1e.

Although it is not shown in this paper, the reader can verify that alignment calibration performance using one star tracker and gyro is essentially the same as with two star trackers and gyro. This is because one star tracker provides three-axis attitude; two star trackers simply improves accuracy. The limited boresight accuracy of a single tracker is not of great consequence when the calibration maneuvers are over a large angular range and at a sufficient angular rate. The reader is invited to verify that this also is true.

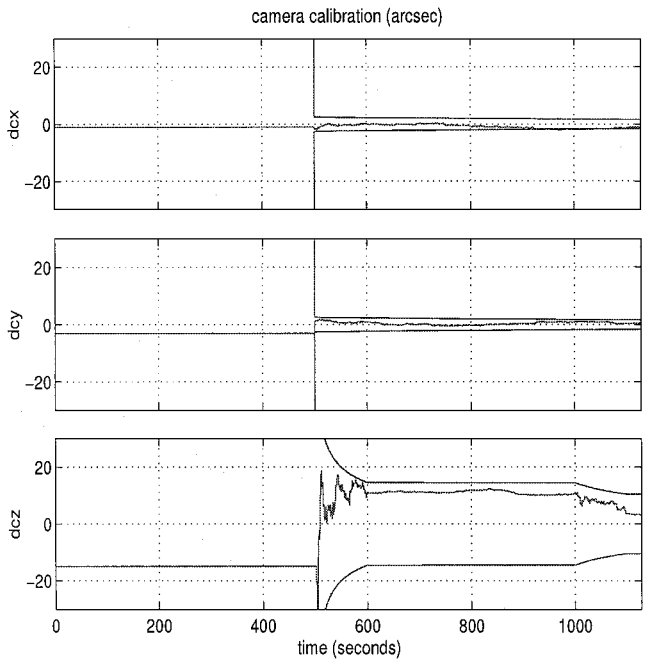

e) Payload alignment estimation error (arc-s)

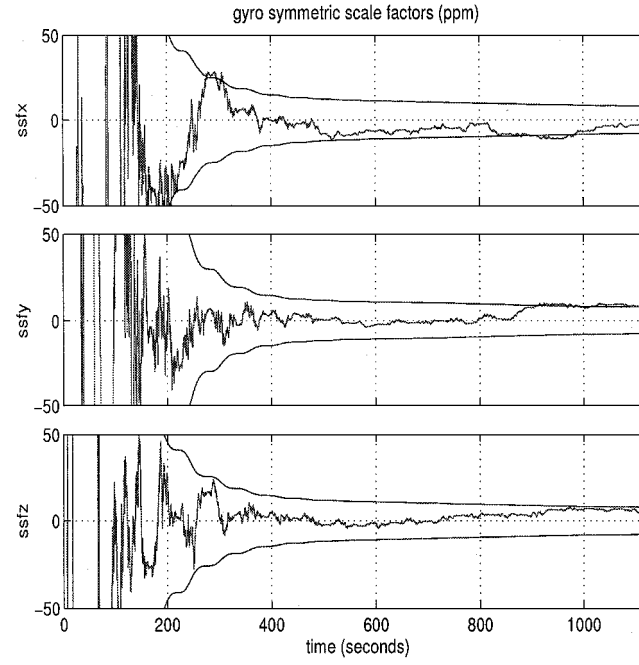

g) Gyro symmetric scale factor estimation error (ppm)

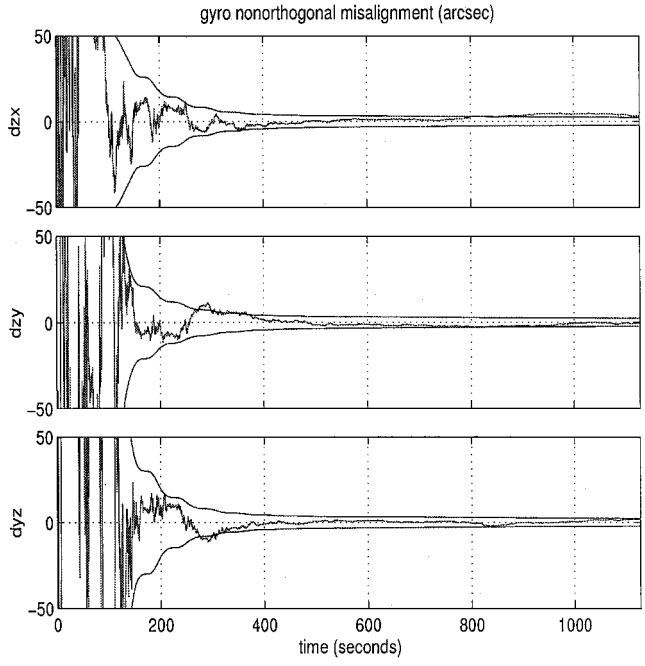

f) Gyro nonorthogonal alignment estimation error (arc-s)

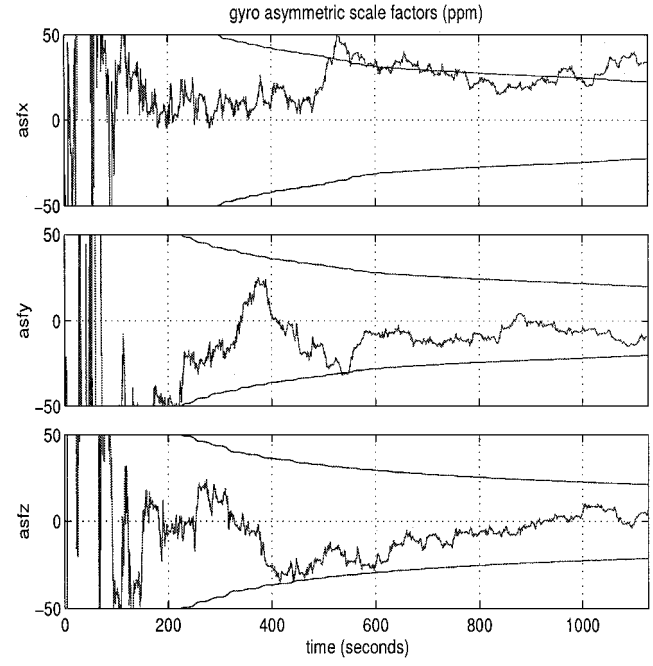

h) Gyro asymmetric scale factor estimation error (ppm)

Fig. 1 Relative alignment calibration results (continued).

Conclusion

We have shown that the absolute alignment error model is a relative alignment error model when measurement data from a reference sensor are used. The reference sensor model does not contain orthogonal misalignment parameters. Because any attitude sensor or gyro can be chosen as the reference sensor, it can be said that everything is relative in system alignment calibration.

The payload has long been considered the source of absolute alignment. A more convenient choice of reference sensor than the payload is the gyro. We defined a model for gyro calibration that includes nonorthogonal misalignment, symmetric scale factor error, and asymmetric scale factor error. The orthogonal misalignment is zero in the gyro misalignment model because the gyro is the reference sensor. We also defined a model for payload alignment calibration and derived its measurement sensitivity equations.

Estimation of payload misalignment is optional in the relative alignment model and can be left strictly to the payload scientists, thus creating a well-defined boundary between ACS calibration and payload calibration. This eliminates potential logistical, communication, and technical problems associated with calibrating the payload alignment as part of the ACS calibration.

Simulation results illustrate the efficacy of the relative alignment model introduced. These results show that the relative alignment and gyro calibration parameters converge without ambiguity. They also show that the payload misalignment can be estimated if necessary.

The relative alignment error model introduced is suitable for autonomous on-orbit real-time calibration because there are no unobservable degrees of freedom in the model. Although few systems have the computational power or the need to do this, there are some high-performance systems that may benefit. A decoupled estimator such as that described in Refs. 5 and 6 may be considered for

this task instead of a full Kalman filter. The first-stage estimator estimates attitude and gyro bias, and the second stage estimates the calibration parameters. The second stage may be updated at a slower rate than the first to save computation time.

Appendix: QS Factorization of the Gyro Misalignment Matrix

The matrix $I + \Delta$ can be factored such that $I + \Delta = \mathcal{Q}\mathcal{S}$, where $\mathcal{Q}$ is orthogonal and $\mathcal{S}$ is symmetric. As before, the matrix $\mathcal{Q}$ is well approximated by a small angle transformation $I + [\delta\times]$. Then

$$I + \Delta = (I + [\delta\times])\mathcal{S} = \begin{bmatrix} 1 & -\delta_z & \delta_y \\ \delta_z & 1 & -\delta_x \\ -\delta_y & \delta_x & 1 \end{bmatrix} \begin{bmatrix} 1 & \zeta_z & -\zeta_y \\ \zeta_z & 1 & \zeta_x \\ -\zeta_y & \zeta_x & 1 \end{bmatrix}$$

$$\simeq \begin{bmatrix} 1 & -(\delta_z - \zeta_z) & \delta_y - \zeta_y \\ \delta_z + \zeta_z & 1 & -(\delta_x - \zeta_x) \\ -(\delta_y + \zeta_y) & \delta_x + \zeta_x & 1 \end{bmatrix} \tag{A1}$$

Equating like terms with the misalignment matrix in Eq. (4) yields the orthogonal and nonorthogonal misalignments in terms of the general misalignments:

$$\delta_x = \tfrac{1}{2}(\delta_{yx} + \delta_{zx}), \qquad \zeta_x = \tfrac{1}{2}(\delta_{yx} - \delta_{zx}) \tag{A2}$$

$$\delta_y = \tfrac{1}{2}(\delta_{xy} + \delta_{zy}), \qquad \zeta_y = \tfrac{1}{2}(\delta_{xy} - \delta_{zy}) \tag{A3}$$

$$\delta_z = \tfrac{1}{2}(\delta_{xz} + \delta_{yz}), \qquad \zeta_z = \tfrac{1}{2}(\delta_{xz} - \delta_{yz}) \tag{A4}$$

Effectively, the nonorthogonal misalignment is split evenly between the body-frame axes. Setting $\delta_x = \delta_y = \delta_z = 0$ gives $I + \Delta = \mathcal{S}$. Note that although there are as many parameters in the symmetric factor S as in the upper triangular factor $\mathcal{R}$, there are fewer multiplications needed to apply $\mathcal{R}$, and so the $\mathcal{Q}\mathcal{R}$ factorization is preferred. From Eq. (A1), we have

$$\begin{bmatrix} 1 & -(\delta_z - \zeta_z) & \delta_y - \zeta_y \\ \delta_z + \zeta_z & 1 & -(\delta_x - \zeta_x) \\ -(\delta_y + \zeta_y) & \delta_x + \zeta_x & 1 \end{bmatrix} \begin{bmatrix} \omega_x \\ \omega_y \\ \omega_z \end{bmatrix}$$

$$= \begin{bmatrix} 0 & \omega_z & -\omega_y & 0 & -\omega_z & \omega_y \\ -\omega_z & 0 & \omega_x & \omega_z & 0 & \omega_x \\ \omega_y & -\omega_x & 0 & \omega_y & -\omega_x & 0 \end{bmatrix} \begin{bmatrix} \delta_x \\ \delta_y \\ \delta_z \\ \zeta_x \\ \zeta_y \\ \zeta_z \end{bmatrix} \tag{A5}$$

The expression on the right is essentially the same as in Ref. 2.

Acknowledgments

The author thanks the reviewers and the Editor-in-Chief for their suggestions on improving the clarity of this paper. Thanks to Dewey Adams, who made a casual remark one day that led me to consider the gyro as the reference sensor in the relative alignment error model.

References

[1]Pittelkau, M. E., "Kalman Filtering Approach to Spacecraft System Alignment Calibration," *Journal of Guidance, Control, and Dynamics*, Vol. 24, No. 6, 2001, pp. 1187–1195.

[2]Davis, S., and Lai, J., "Attitude Sensor Calibration for the Ocean Topography Experiment Satellite," *SPIE Space Guidance, Control, and Tracking Conference*, Vol. 1949, Society of Photo-Optical Instrumentation Engineers, Bellingham, WA, 1993, pp. 80–91.

[3]Deutschmann, J., and Bar-Itzhack, I. Y., "Extended Kalman Filter for Attitude Estimation of the Earth Radiation Budget Satellite," *Flight Mechanics and Estimation Theory Symposium*, NASA CP-3050, May 1989, pp. 333–345.

[4]Murrell, J. W., "Precision Attitude Determination for Multimission Spacecraft," *Proceedings of the AIAA Guidance and Control Conference*, AIAA, New York, 1978, pp. 70–87.

[5]Zanardi, M. C., and Shuster, M. D., "Batch and Filter Approaches to Spacecraft Sensor Alignment Estimation," *12th International Symposium on Spaceflight Dynamics*, ESA Publ. Div., Noordwijk, The Netherlands, 1997, pp. 171–177.

[6]Shuster, M. D., "Inflight Estimation of Spacecraft Sensor Alignment," *13th Annual AAS Guidance and Control Conference*, American Astronautical Society, 1990, pp. 253–274.

[7]Shuster, M. D., Pitone, D. S., and Bierman, G. J., "Batch Estimation of Spacecraft Sensor Misalignments, I. Relative Alignment Estimation," *Journal of the Astronautical Sciences*, Vol. 39, No. 4, 1991, pp. 519–546.

[8]Shuster, M. D., and Pitone, D. S., "Batch Estimation of Spacecraft Sensor Misalignments, II. Absolute Alignment Estimation," *Journal of the Astronautical Sciences*, Vol. 39, No. 4, 1991, pp. 547–571.

[9]Shuster, M. D., and Lopes, R. V. F., "Parameter Interference in Distortion and Alignment Calibration," American Astronautical Society, AAS Paper 94-186, Feb. 1994.

[10]Davenport, P., and Welter, G., "Algorithm for In-Flight Calibration of Gyros," *Flight Mechanics/Estimation Theory Symposium*, NASA CP-3011, May 1988, pp. 114–127.

[11]Lefferts, E. J., Markley, F. L., and Shuster, M. D., "Kalman Filtering for Spacecraft Attitude Estimation," *Journal of Guidance, Navigation, and Control*, Vol. 5, No. 5, 1982, pp. 417–429.

[12]Jazwinski, A. H., "Stochastic Processes and Filtering Theory," *Mathematics in Science and Engineering*, Vol. 64, Academic Press, New York, 1970, pp. 305, 306.

[13]Pittelkau, M. E., "A Factorization and Least-Squares Method for Multi-Pass Sensor Alignment Calibration," American Astronautical Society, AAS Paper 01-151, Feb. 2001.

D. B. Spencer
Associate Editor